RCS Reduction of Canonical Targets Using Genetic Algorithm Synthesized RAM

Hossein Mosallaei, *Student Member, IEEE*, and Yahya Rahmat-Samii, *Fellow, IEEE*

***Abstract*—Radar cross section (RCS) reduction of canonical (planar, cylindrical, and spherical) conducting targets is the focus of this paper. In particular, a novel procedure is presented for synthesizing radar absorbing materials (RAM) for RCS reduction in a wide-band frequency range. The modal solutions of Maxwell's equations for the multilayered planar, cylindrical, and spherical canonical structures is integrated into a genetic algorithm (GA) optimization technique to obtain the best optimal composite coating. It is shown that by using an optimal RAM, the RCS of these canonical structures can be significantly reduced. Characteristics of bistatic RCS of coated cylindrical and spherical structures are also studied and compared with the conducting structures without coating. It is shown that no optimal coating can be found to reduce the RCS in the deep shadow region. An in-depth study has been performed to evaluate the potential usage of the optimal planar coating as applied to the curved surfaces. It is observed that the optimal planar coating can noticeably reduce the RCS of the spherical structure. This observation was essential in introducing a novel efficient GA with hybrid planar/curved surface implementation using as part of its initial generation the best population obtained for the planar RAM design. These results suggest that the optimal RAM for a surface with arbitrary curvature may be efficiently determined by applying the GA with hybrid planar/curved surface population initialization.**

***Index Terms*—Canonical structures, electromagnetic scattering by absorbing media, genetic algorithms (GAs), radar absorbing materials (RAM), radar cross section (RCS), radar scattering.**

I. Introduction

RADAR cross section (RCS) reduction of a target using multilayered radar absorbing materials (RAM) has been an important consideration in radar systems [1], [4]. In complex structures, for example a fighter plane, one can identify canonical features composed of planar, cylindrical, and spherical surfaces as shown in Fig. 1. In designing RAM, it becomes important to obtain an optimized RAM for reducing the RCS of these canonical structures. It is also of interest to investigate the usefulness of the optimal planar RAM for RCS reduction in curved structures. These issues are addressed in this paper by utilizing the power of mode matching technique integrated with a novel utilization of an efficiently implemented GA optimizer [5]. Fig. 1 provides the key features of this implementation.

Modal solutions of Maxwell's equations for the multilayered coated canonical targets, as depicted in Fig. 1, are used as the main computational engine for the accurate and efficient computations of scattered fields. In the spirit of the theme of this special issue being dedicated to the memory of Prof. Wait, considerable attention is given to Prof. Wait's pioneering contributions. The list of references demonstrates the nature of his contributive efforts in the area of multilayered canonical structures [6]–[29]. Next, the genetic algorithm (GA) optimization technique is applied to obtain the optimal RAM for reducing RCS of coated structures. This is an excellent example in demonstrating how the classical analytical solutions can be advantageously used with modern optimization techniques for the determination of an optimal design.

The design of optimal coating for reducing the reflection coefficient of planar structures was investigated by Michielssen *et al.* [2]. The present paper extends their methodology to reduce the RCS of curved surfaces, including cylindrical and spherical structures, and it attempts to provide useful design guidelines and physical observations. Since, in general, properties of the RAM depend on the frequency for wide-band absorption, a proper composite selection of these materials is necessary. The GA is an effective optimizer to obtain the best combination of the RAM among available database of materials. The GA is successfully applied to the synthesis of wide-band absorbing coating in a specified frequency range. It is observed that by a proper selection of materials and their thickness, the target's RCS is reduced significantly. The bistatic RCS of coated conducting cylindrical and spherical structures are also determined. It is observed that even though the optimal RAM was designed for reducing the monostatic RCS, the bistatic RCS are also reduced significantly in the lit region. It is further shown that in the deep shadow region the RCS cannot be reduced no matter how effectively the optimization process is applied. This is, of course, a very important observation. Additionally, the effectiveness of the optimal planar coating for RCS reduction in a structure with arbitrary curvature is demonstrated. This observation was essential in introducing a novel efficient GA implementation using as part of its initial generation the best population obtained for the planar RAM design.

The main features of this paper in designing the optimal RAM coating are summarized in the following:

- integrating the *GA* optimizer with the *modal solutions* of Maxwell's equations for the canonical structures;
- developing an *efficient GA* for obtaining the optimal RAM for *curved surfaces* based on the utilization of the optimal planar coating as the initial population;
- presenting *optimized RAM* coating for significant RCS reduction;
- investigating *Bistatic RCS reduction* and addressing the important issue of the *deep shadow* region;

Manuscript received August 31, 1999; revised April 6, 2000.

The authors are with the Department of Electrical Engineering, University of California at Los Angeles, Los Angeles, CA 90095-1594 USA (e-mail: rahmat@ee.ucla.edu).

Publisher Item Identifier S 0018-926X(00)09353-4.

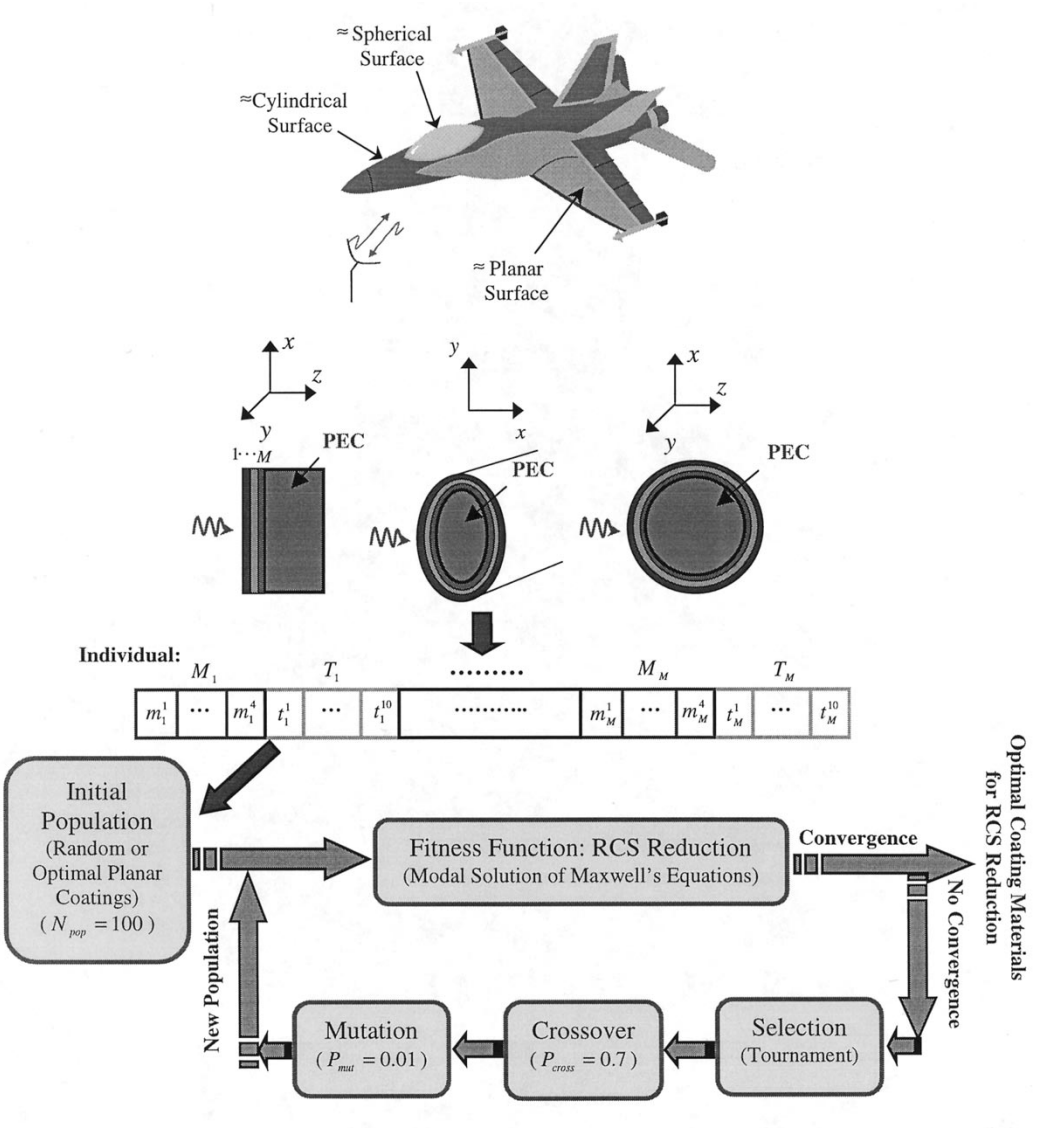

Fig. 1. Flowchart of the GA integrated with the modal solution of Maxwell's equations for obtaining optimal RAM. Note the possibility of using GA planar/curved surface implementation for initializing the population. Coated planar, cylindrical, and spherical targets with their appropriate coordinate systems are also shown.

- providing *useful insights* for proper interpretations of the optimal results.

In the following section, the GA optimization technique integrated with the modal solutions of Maxwell's equations for canonical structures is summarized. Section III investigates a wide-band absorbing coating for the planar structures. In Section IV, monostatic and bistatic RCS, and the deep shadow region of coated cylindrical and spherical structures are studied and characterized. In Section V, RCS reduction of curved surfaces using an efficient implementation of GA technique is highlighted. Finally, Section VI provides some concluding remarks.

II. Integration of the Genetic Algorithm and Modal Solutions

A. GA Implementation

The GAs are iterative optimization procedures that typically start with a randomly selected population of solution domain and gradually evolve toward better solution through the application of genetic operators that are selection, crossover, and mutation [5]. GAs are global optimizers and could be an efficient technique for optimizing the new electromagnetic problems having discontinuous and constrained parameters, discrete solution domain, and a large number of dimensions with many local optima [30].

In the context of obtaining M-layered wide-band absorbing coating for reducing RCS of a conducting structure, the objective or fitness function F is defined by

$$F(M_1, T_1, M_2, T_2, \ldots, M_M, T_M) = \text{Min}\left[\text{RCS}^{(\text{dB})}_{\text{conductor}} - \text{RCS}^{(\text{dB})}_{\text{coated}}\right]\Big|_{\{f_1, f_2, \ldots, f_{N_f}\}} \quad (1)$$

where M_j and T_j represent the material choice and thickness of the jth layer, respectively. Application of (1) as a fitness function for GA is an attempt to maximize the minimum difference between the RCS (in decibels) of the original target and the RAM coated one in the desired frequency band. In this study, a

TABLE I
RELATIVE PERMITTIVITIES AND PERMEABILITIES OF THE 16 MATERIALS IN THE DATABASE [2]

Lossless Dielectric Materials ($\mu_r = 1. - j0.$)		
#	ε_r	
1	$10. - j0.$	
2	$50. - j0.$	
Lossy Magnetic Materials ($\varepsilon_r = 15. - j0.$)		
$\mu = \mu_r - j\mu_i,\ \mu_r(f) = \mu_r(1GHz)/f^{\alpha},\ \mu_i(f) = \mu_i(1GHz)/f^{\beta},\ (f\ in\ GHz)$		
#	$\mu_r(1GHz), \alpha$	$\mu_i(1GHz), \beta$
3	5., 0.974	10., 0.961
4	3.,1.000	15., 0.957
5	7., 1.000	12., 1.000
Lossy Dielectric Materials ($\mu_r = 1. - j0.$)		
$\varepsilon = \varepsilon_r - j\varepsilon_i,\ \varepsilon_r(f) = \varepsilon_r(1GHz)/f^{\alpha},\ \varepsilon_i(f) = \varepsilon_i(1GHz)/f^{\beta},\ (f\ in\ GHz)$		
#	$\varepsilon_r(1GHz), \alpha$	$\varepsilon_i(1GHz), \beta$
6	5., 0.861	8., 0.569
7	8., 0.778	10., 0.682
8	10., 0.778	6., 0.861
Relaxation-type Magnetic Materials ($\varepsilon_r = 15 - j0.$)		
$\mu = \mu_r - j\mu_i,\ \mu_r(f) = \frac{\mu_m f_m^2}{f^2 + f_m^2},\ \mu_i(f) = \frac{\mu_m f_m f}{f^2 + f_m^2},\ (f\ and\ f_m\ in\ GHz)$		
#	μ_m	f_m
9	35.	0.8
10	35.	0.5
11	30.	1.0
12	18.	0.5
13	20.	1.5
14	30.	2.5
15	30.	2.0
16	25.	3.5

small database containing 16 different materials with permittivities $\varepsilon_i(f)$ and permeabilities $\mu_i(f)$, as shown in Table I, is considered [2]. The design goal is to determine an optimal M-layered coating in order to maximize the minimum RCS reduction in a prescribed range of frequencies $\{f_1, f_2, \ldots, f_{N_f}\}$.

In order to apply the GA method to a multilayered coated conducting structure (planar, cylindrical, and spherical structure), material and thickness of jth layer are represented in the finite sequences of binary bits as

$$L_j = M_j T_j = [m_j^1 m_j^2 \ldots m_j^{N_{mb}}][t_j^1 t_j^2 \ldots t_j^{N_{tb}}]. \qquad (2)$$

The entire structure is subsequently represented by the sequence $G = L_1 L_2 \ldots L_M$. The database includes 16 different available materials that can be represented by four binary bits or $N_{mb} = 4$. In addition, for designing the thickness of each layer with three-digit resolution, each layer is represented by ten binary bits with $N_{tb} = 10$. In the process of the GA implementation, a population with size $N_{pop} = 100$, crossover with $p_{cross} = 0.7$, and mutation with $p_{mut} = 0.01$ are used [30]–[32]. Additionally, the tournament selection and elitism are employed in the process of creating the new generation. Tracking the performance of the best sequence in the population, as well as the average performance of all sequences checks the convergence of the algorithm. If no improvement in both quantities in a large number of generations occurs, the procedure is assumed to have converged. The optimization procedure is shown in Fig. 1.

For certain applications, the coating should not only absorb the incident wave in a wide range of frequency, but should also be as light as possible. Therefore, in the cases studied in this paper, five-layer coating ($M = 5$) with thickness $0 \leq t_i(\text{cm}) \leq 0.2$ is used. The GA is successfully applied to the synthesis of a wide-band coating in the typical frequency range $0.2 \leq f(\text{GHz}) \leq 2$ by sampling the cost function F at ten different frequency points $N_f = 10$.

Based on our experience in obtaining the optimal RAM for the cylindrical and spherical structures, about 100 generations containing 100 individuals are necessary. Additionally, the RCS for each individual has to be computed at ten different frequency points. A GA implementation with a particular selection of initial population has proven to provide rapid convergence. In this implementation, the best population for the planar coating initializes the GA process for the optimal RAM design of curved structures. Section V will highlight some of the unique features of this implementation.

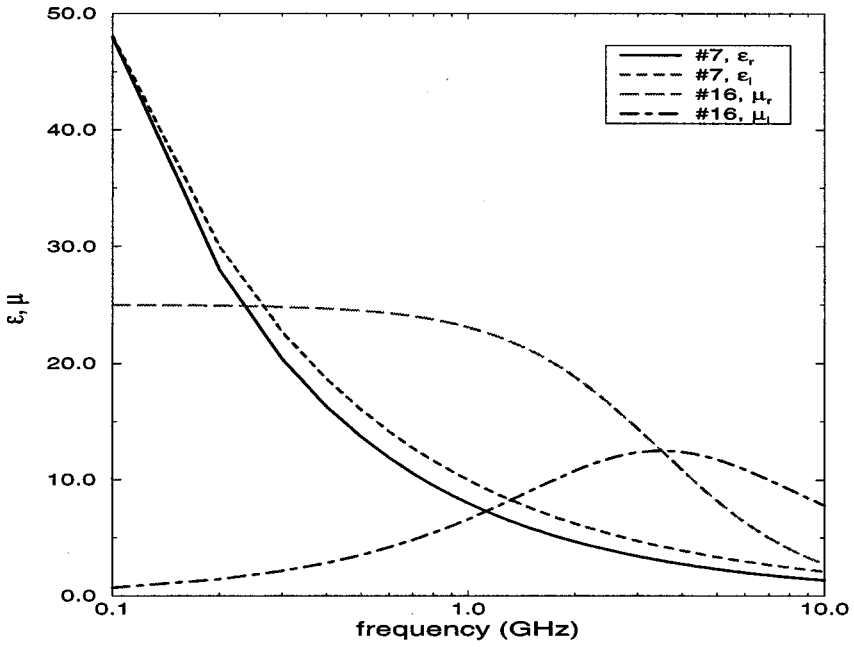

Fig. 2. Relative permittivity and permeability of materials #7 and #16, from Table I, as a function of frequency.

B. Modal Solutions of Maxwell's Equations for Canonical Structures

In this section, the underlying electromagnetic formulations for the scattered fields of the canonical structures are briefly summarized. Fig. 1 depicts the M-layered coated conducting planar, cylindrical, and spherical structures, illuminated by a normally incident plane wave. The choice of the normal incidence was primarily made in order to provide a common base for comparing the results of various target shapes. The monostatic RCS of these canonical structures are evaluated at normal incidence. The total electric field in the presence of the coated structure is written as

$$\mathbf{E} = \mathbf{E}^i + \mathbf{E}^s \tag{3}$$

where $\mathbf{E}^i$ and $\mathbf{E}^s$ are the incident and scattered field, respectively. The scattered field $\mathbf{E}^s$ for these canonical structures is obtained using the modal solutions of the Maxwell's equations. Based on the geometry, the modal solution is represented as a plane wave, cylindrical wave, or spherical wave functions. Next, by applying the boundary conditions and utilizing an accurate computer code, the electromagnetic fields for these canonical structures are obtained.

It is noted that one of the properties of the radar absorbing materials is that their relative permittivity and permeabilty are a complex-valued function of frequency. The presence of this type of materials, often with a large imaginary part, forces one to pay increased attention in the evaluation of the Bessel and Hankel functions for the cylindrical and spherical structures. Note that over the frequency range of interest, the diameter of the cylindrical and spherical structures varies between about $1\ \lambda - 25\ \lambda$. For instance, in some of the RAM coatings, the Bessel functions with a large argument value around 1100 have to be computed. In addition, we analyze a multilayered structure that makes the computational technique more complex. The computer program is a double precision code, which uses an efficient Bessel and Hankel functions computation [33], [34] for accurate determination of the scattered fields. The program internally checks the convergence of the electromagnetic fields and selects the required number of summation terms. Its accuracy has been tested against numerous available published data [1], [35].

III. Wide-Band Absorbing Coating for Planar Structures

In this section the GA optimization technique is integrated with the modal solutions in order to obtain the best combinations of the RAM coating for planar structures, in a wide!band of frequency. The reflection coefficient is determined as

$$\Gamma = \frac{|\mathbf{E}^s|}{|\mathbf{E}^i|}. \tag{4}$$

In this study, the reflection coefficient is minimized only for normal incidence. As mentioned earlier, the available RAM is summarized in Table I; although these materials are fictitious, they provide a good representative sample of a wide class of available RAM. The characteristics of these materials can be categorized in the following ways [2].

1) Lossless and frequency-independent dielectric materials (#1–2).
2) Lossy magnetic (#3–5) and lossy dielectric (#6–8) materials. These materials are frequency-dependent with f in GHz as defined in Table I.
3) Lossy magnetic with a relaxation type characteristic materials (#9–16). These materials are also frequency-dependent with f in gigahertz, as represented in Table I.

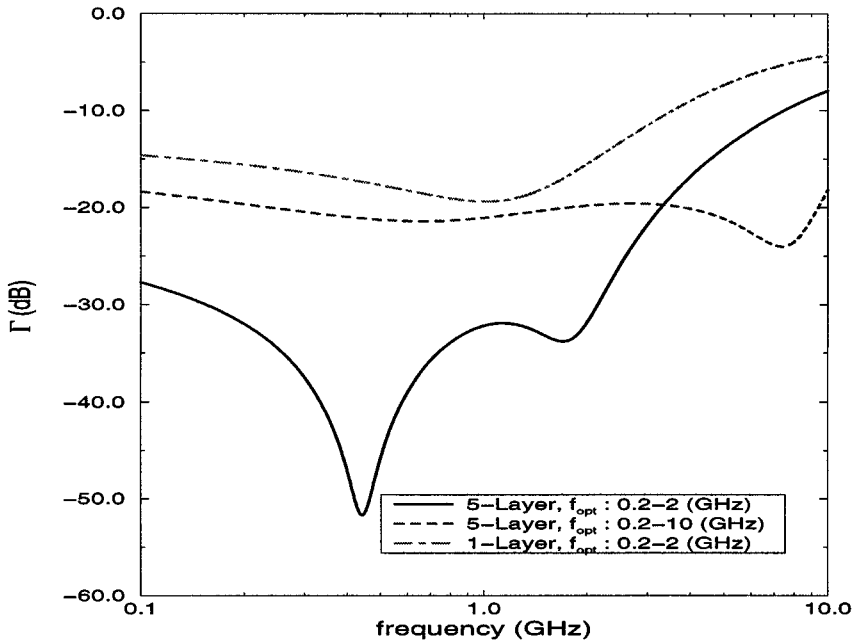

Fig. 3. Reflection coefficient of the RAM coated conducting planar structure . (Note that $\Gamma = 0.$ dB for the PEC.)

TABLE II
OPTIMUM RAM FOR THE CONDUCTING PLANE. (a) $0.2 \leq f_{\rm opt}(\rm GHz) \leq 2$ (b) $0.2 \leq f_{\rm opt}(\rm GHz) \leq 10$

Layer	Material #	$t\,(cm)$
1	14	0.0888
2	6	0.143
3	4	0.0559
4	4	0.166
5	4	0.154

(a)

Layer	Material #	$t\,(cm)$
1	14	0.0434
2	6	0.177
3	5	0.140
4	4	0.193
5	2	0.0649

(b)

As an example, the relative permittivity and permeability of materials #7 and #16 are plotted in Fig. 2. As seen, these materials have different characteristics as a function of frequency. Application of GA method allows one to obtain the best selection of the available RAM (Table I) in the desired range of frequency.

The optimal planar coatings for reducing the reflection coefficient of the conducting planar structure, illuminated at normal incidence, are shown in Table II. In this case, two optimization frequency ranges, namely, 0.2–2 GHz at ten points and 0.2–10 GHz at 20 points are studied. Reflection coefficient of the coated structure is shown in Fig. 3 and it reveals a good agreement with the published data by Michielssen *et al.* [2]. As observed, the RAM coating decreases the reflection coefficient about 32 dB for the first optimization range. For optimization range of 0.2–10 GHz, the reflection coefficient is almost flat and it is reduced by about 18 dB.

One may wonder what happens if the GA optimizer is allowed to use only a single material during the optimization process. The effect of using a single layer coating in reducing the reflection coefficient of the planar structure in the frequency range 0.2–2 GHz is presented in Fig. 3. The thickness of the coating is allowed to change between $0 \leq t_1(\rm cm) \leq 1$ in the GA procedure. The optimal RAM is the material #4 with thickness $t_1 = 0.249$ cm. It shows that based on these materials, using one coating only reduces the reflection coefficient about 15 dB in the optimization frequency range.

The most difficult part in reducing the reflection coefficient of the planar structure occurs at very low frequency. In this range of frequency, the finite conductivity in most of the available materials makes the coating act like a perfect conductor and the energy cannot enter the coating to be absorbed [36]. At high frequencies around 10 GHz, the relative permittivity and permeability of the materials are decreased and they cannot control the reflection coefficient of the structure effectively. Using a more effective available database, and increasing number of layers and their thickness can further reduce the reflection coefficient.

IV. RCS REDUCTION FOR CYLINDRICAL AND SPHERICAL STRUCTURES

A. Monostatic RCS Reduction

In this section, the GA is applied to synthesize a wide-band absorbing RAM in the frequency range of 0.2–2 GHz, for monostatic RCS reduction of conducting cylindrical and spherical

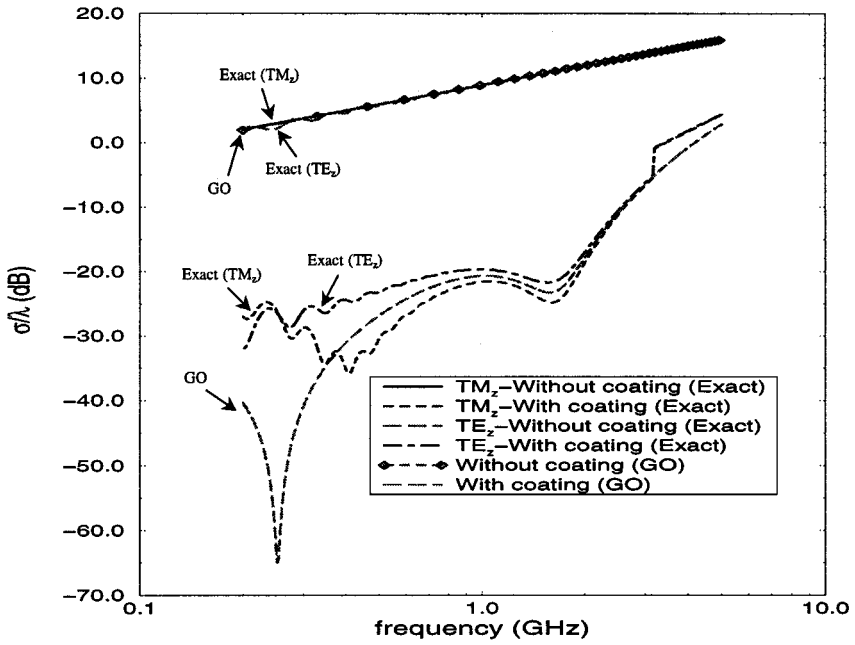

Fig. 4. RCS of the conducting cylinder, without and with coating. (Diameter of the cylinder varies between $1\ \lambda - 10\ \lambda$ in the optimized frequency range of 0.2–2 GHz.) RCS based on GO formula is also shown.

structures. In the cases studied here, the optimal RAM is determined for representative conducting structures with 148 cm diameter (electric size is changed from about $1\ \lambda - 10\ \lambda$ in the optimization range $0.2 \leq f \leq 2$ GHz).

For a cylindrical structure, the RCS for TM_z mode is obtained using the definition of two-dimensional (2-D) RCS as

$$\sigma_{2-D} = \lim_{\rho \to \infty} \left[2\pi\rho \frac{|\mathbf{E}^s|^2}{|\mathbf{E}^i|^2} \right]. \tag{5}$$

RCS for TE_z case is similarly determined. The corresponding coatings and their thickness are presented in Table III(a). In the optimization procedure one could use TM_z or TE_z modes separately; however, from practical consideration, the optimum coating is determined for both polarizations simultaneously. Fig. 4 displays the RCS of the conducting cylinder, without and with coating for both TM_z and TE_z modes. It is observed that the optimal absorbing materials reduce the RCS of the conducting cylinder by about 27 dB in the optimization frequency range. In the resonance region, the optimal coating works very well as an absorber; and as one extends the solution to the Rayleigh region, it is found that this effect is reduced. At the low frequencies, most of the materials act as a perfect conductor, and the coating cannot absorb the energy of the incident wave as well as in the resonance region. Additionally, at the higher frequency range, the relative permittivity and permeability of the materials are reduced and the RCS cannot be reduced effectively.

Fig. 4 also shows the RCS of the coated cylindrical structure based on the geometrical optics (GO) formula as [37]

$$\sigma_{2-D} = |\Gamma_{\text{cylinder}}|^2 \cdot \pi a_{\text{coated}} \tag{6}$$

TABLE III
OPTIMUM RAM FOR THE 148 CM DIAMETER CONDUCTING CYLINDER. $(0.2 \leq f_{\text{opt}}(\text{GHz}) \leq 2)$ (a) MONOSTATIC $(\phi = 180^\circ)$ (b) BISTATIC $(\phi = 0^\circ)$

Layer	Material #	t (cm)
1	15	0.0968
2	7	0.123
3	4	0.197
4	7	0.0195
5	4	0.191

(a)

Layer	Material #	t (cm)
1	2	0.0163
2	8	0.0109
3	8	0.0104
4	1	0.0100
5	8	0.0139

(b)

where Γ_{cylinder} is the reflection coefficient of the planar structure coated with the optimal cylindrical coating [Table III(a)], and a_{coated} is the outer radius of the coated cylindrical structure. Good agreement between the modal solution and GO approximation is observed.

For the spherical target the RCS is obtained as

$$\sigma_{3-D} = \lim_{r \to \infty} \left[4\pi r^2 \frac{|\mathbf{E}^s|^2}{|\mathbf{E}^i|^2} \right]. \tag{7}$$

The optimal RAM coating for reducing the RCS of the conducting sphere in the optimization frequency range of 0.2–2 GHz is shown in Table IV(a). The RCS has been plotted in

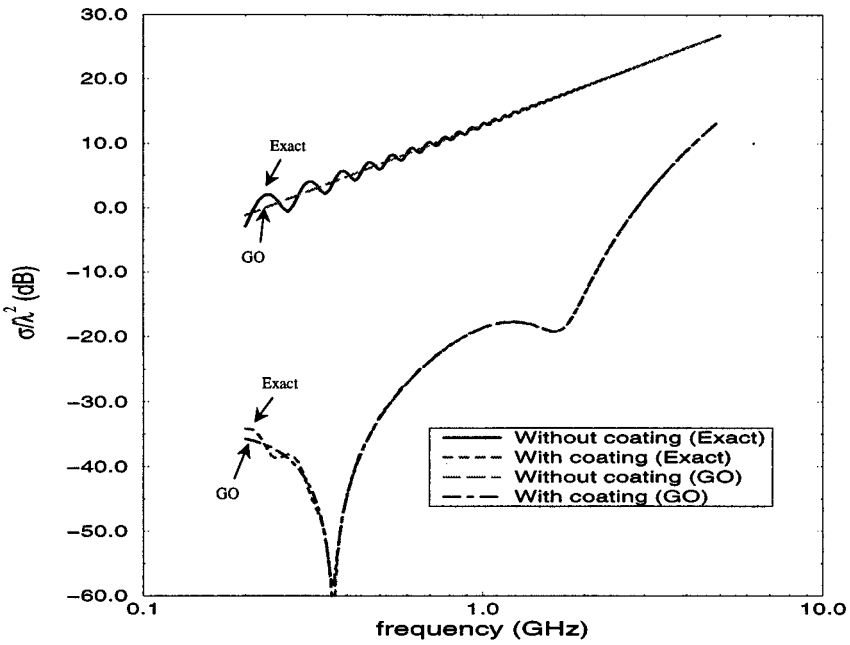

Fig. 5. RCS of the conducting sphere, without and with coating. (Diameter of the sphere varies between $1\ \lambda - 10\ \lambda$ in the optimized frequency range of 0.2–2 GHz.) RCS based on GO formula is also shown.

TABLE IV
OPTIMUM RAM FOR THE 148 CM DIAMETER CONDUCTING SPHERE. $(0.2 \leq f_{\rm opt}(\text{GHz}) \leq 2)$ (a) MONOSTATIC $(\theta = 180°)$ (b) BISTATIC $(\theta = 0°)$

Layer	Material #	$t\,(cm)$
1	14	0.0962
2	7	0.115
3	4	0.194
4	4	0.188
5	6	0.150

(a)

Layer	Material #	$t\,(cm)$
1	16	0.0652
2	8	0.0113
3	1	0.0104
4	1	0.0111
5	16	0.0250

(b)

Fig. 5. As observed, the optimum coating reduces the RCS of the conducting sphere by about 31 dB in the optimization frequency range. In the resonance region, the optimal coating is a very good absorber and as one extends into the Rayleigh region due to the finite conductivity nature of the materials considered in this study, the RCS of the structure cannot be reduced as well as in the resonance region. In addition, at the higher frequencies, as mentioned earlier, the RCS cannot be controlled effectively.

Fig. 5 also shows the RCS computation based on the geometrical optics formula as [37]

$$\sigma_{3-D} = |\Gamma_{\rm sphere}|^2 \cdot \pi a_{\rm coated}^2 \tag{8}$$

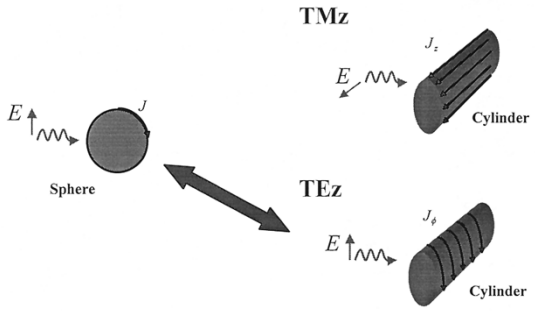

Fig. 6. Current distributions on the cylindrical structure for TM_z and TE_z modes, compared with the spherical structure. Note the surface current flow on the cylindrical structure for TE_z mode has closer similarity to the nature of the current flow on the spherical structure.

where $\Gamma_{\rm sphere}$ is the reflection coefficient from the planar structure using the optimized spherical coating [Table IV(a)], and $a_{\rm coated}$ is the outer radius of the coated spherical structure. It is observed that the computational results for the frequencies above 0.3 GHz closely resemble the results obtained using the GO formula.

As noted from Fig. 5, the RCS for the spherical structure is more similar to the RCS of the cylindrical structure for TE_z mode (Fig. 4). The reason is that for TE_z case the surface current, as shown in Fig. 6, is in the ϕ direction, and it shows similarity to the current direction on the spherical geometry. However, in TM_z case the current is in the z direction (Fig. 6) and does not resemble any current distribution on the spherical surface.

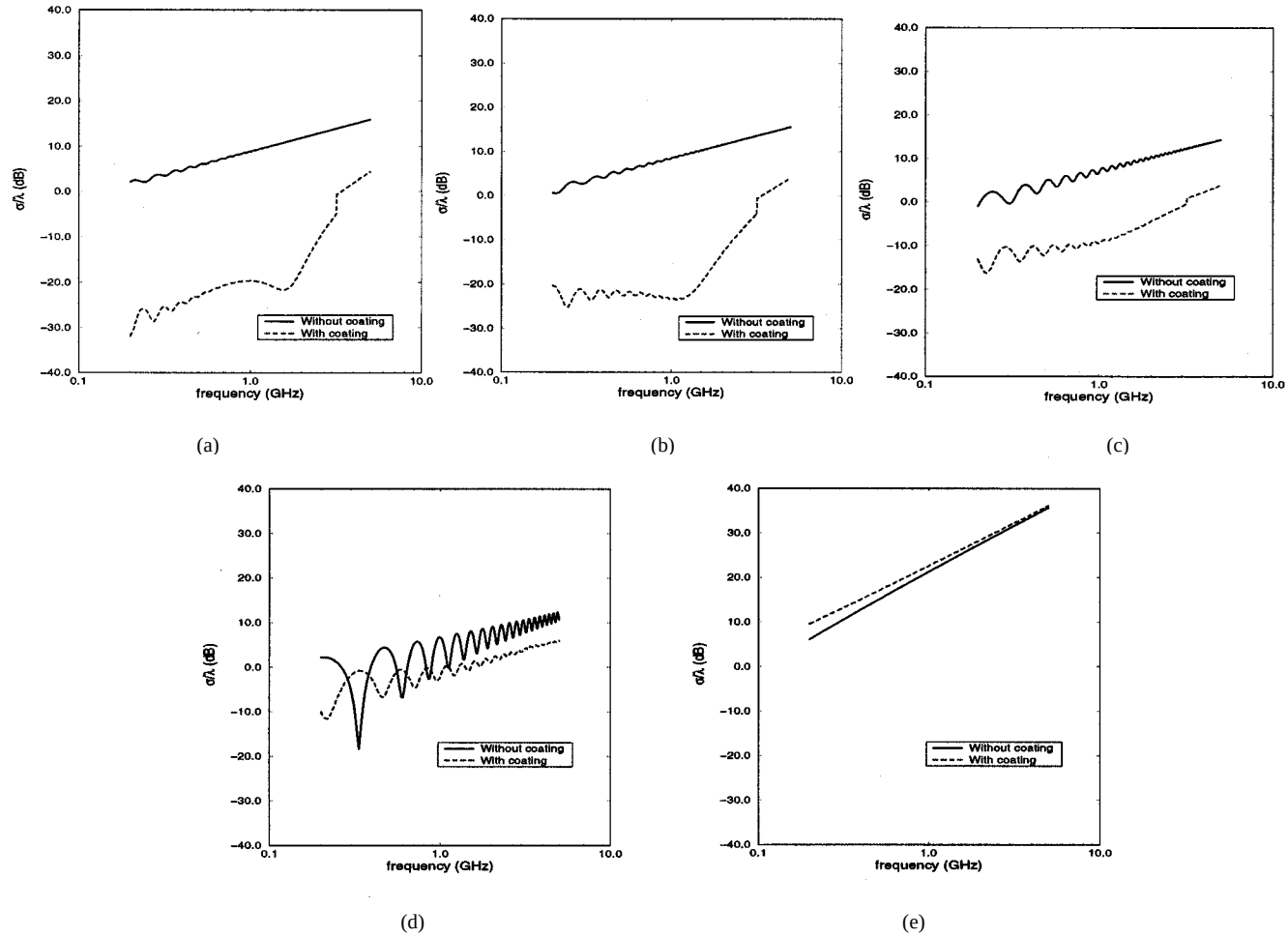

Fig. 7. Bistatic RCS of the conducting cylinder (TE_z case), without and with coating [Table III(a)]. (Diameter of the cylinder varies between $1\ \lambda - 10\ \lambda$ in the optimized frequency range of 0.2–2 GHz.) (a) $\phi = 180°$ (monostatic). (b) $\phi = 135°$. (c) $\phi = 90°$. (d) $\phi = 45°$. (e) $\phi = 0°$ (forward scattering).

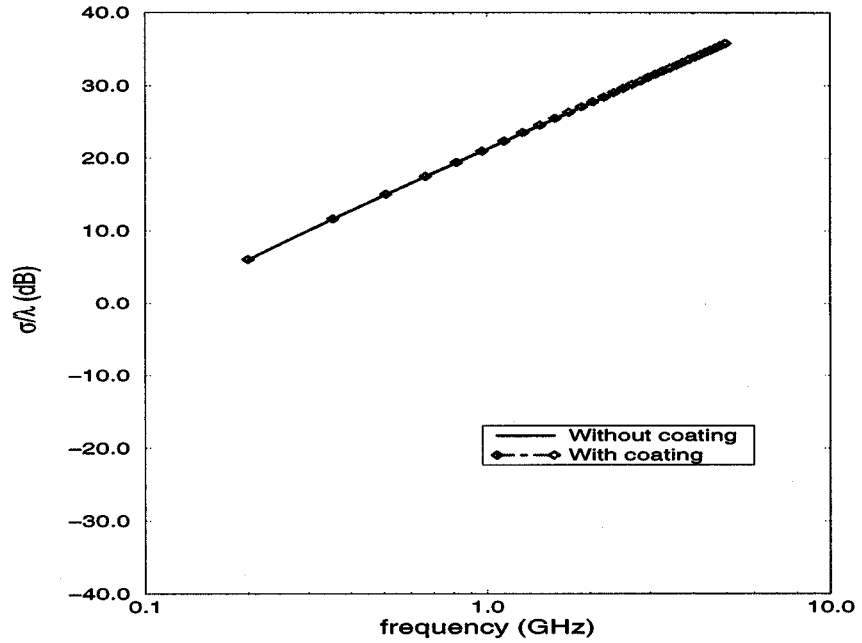

Fig. 8. Bistatic RCS of the conducting cylinder (TE_z case) in the deep shadow region ($\phi = 0°$), without and with coating [Table III(b)]. (Diameter of the cylinder varies between $1\ \lambda - 10\ \lambda$ in the optimized frequency range of 0.2–2 GHz.)

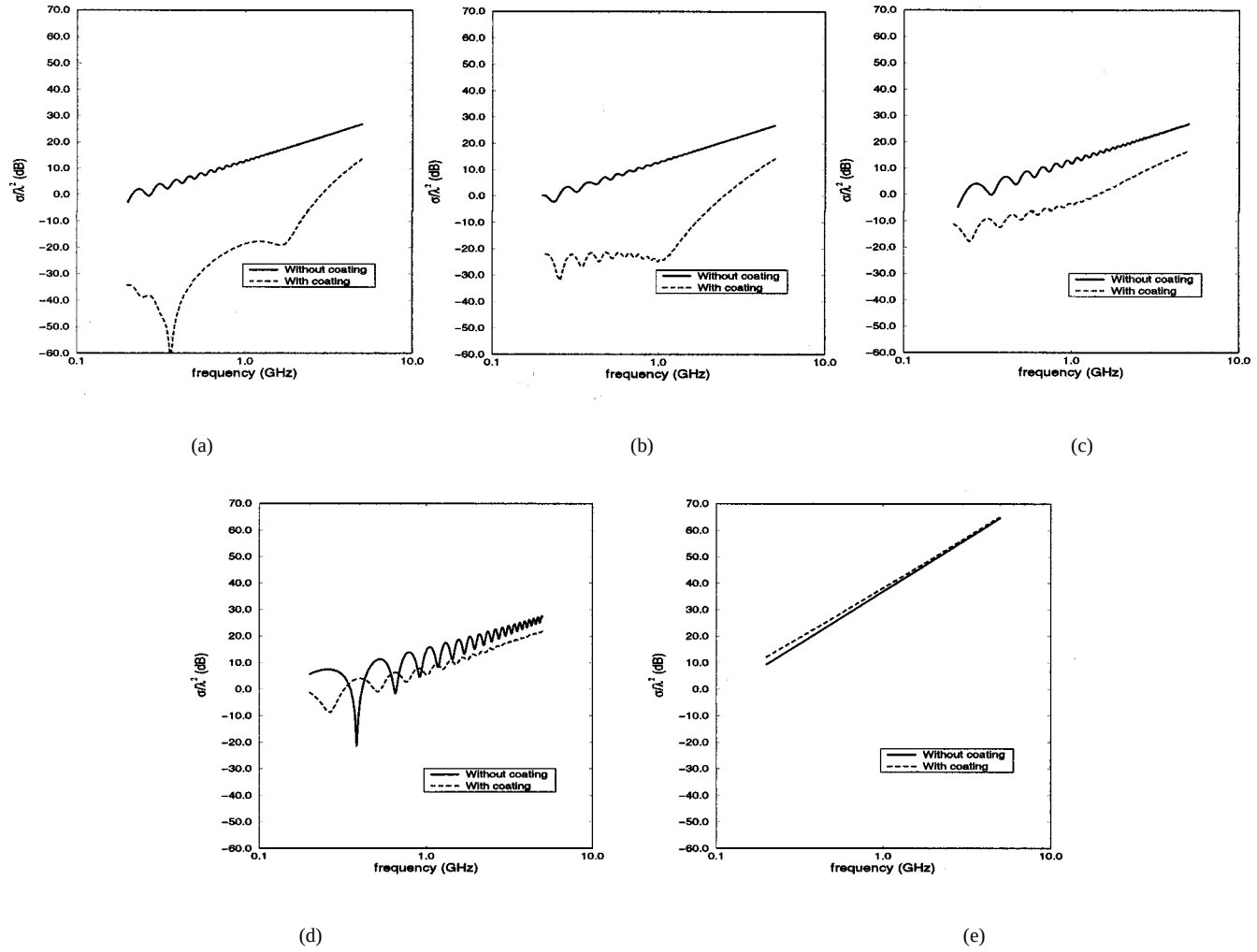

Fig. 9. Bistatic RCS of the conducting sphere (E-plane), without and with coating [Table IV(a)]. (Diameter of the sphere varies between $1\ \lambda - 10\ \lambda$ in the optimized frequency range of 0.2–2 GHz.) (a) $\theta = 180°$ (monostatic). (b) $\theta = 135°$. (c) $\theta = 90°$. (d) $\theta = 45°$. (e) $\theta = 0°$ (forward scattering). In order to show the range of RCS variations, the dynamic range in these plots varies from -60 to 70 dB in contrast to the cylindrical case with an 80-dB dynamic range (Fig. 7).

B. Bistatic RCS Reduction and the Deep Shadow Region

As mentioned earlier, the optimal coating is obtained for reducing the monostatic RCS. The effect of the coating on RCS of the conducting cylinder in other directions is presented in Fig. 7. In this figure, the bistatic RCS of the cylindrical structure with and without coating, for TE_z case, in different directions $\phi = 180°$ (monostatic), $135°$, $90°$, $45°$, and $0°$ (forward scattering) are shown. As observed, the bistatic RCS in the lit region as well as the monostatic RCS is strongly reduced. Additionally, it also follows the GO formula (6) in the lit region. Although the optimal coating is achieved for reducing the monostatic RCS due the existence of lossy materials, this coating also reduces the RCS in other directions expect in the deep shadow region. This can be explained by recognizing the fact that in the deep shadow region the scattered field is usually 180° out of phase with the incident field and so there should be a high level of scattered field, no matter which type of composite coating is used. Note that at low frequencies, as mentioned earlier, the coating is almost the same as a perfect conductor and it only increases the size of the cylinder.

To further evaluate the possibility of RCS reduction in the deep shadow region, an optimization was performed to specifically reduce the bistatic RCS of the conducting cylinder in the deep shadow direction ($\phi = 0$). Table III(b) shows the optimal materials for this trial. The bistatic RCS in the deep shadow region is plotted in Fig. 8 and it reveals that even this optimal coating cannot reduce the RCS in the deep shadow region. For TM_z case, similar observations for the bistatic RCS are obtained.

Bistatic RCS of the conducting sphere, coated with the optimal RAM for reducing the monostatic RCS [Table IV(a)] is investigated in Fig. 9. The bistatic RCS is plotted in E-plane for different elevation angles $\theta = 180°$(monostatic), $135°$, $90°$, $45°$, and $0°$ (forward scattering). Due to the existence of lossy materials, the bistatic RCS in the lit region as well as the monostatic RCS is reduced considerably. However, similar to the cylindrical structure, in the deep shadow region the scattered field is 180° out of phase with the incident wave and there is a high level of scattered field, as shown in Fig. 9(e). Table IV(b) and Fig. 10 show the optimal RAM and bistatic RCS of the spherical structure in the deep shadow region ($\theta = 0°$), and as mentioned, the optimal coating only increase the size of the sphere

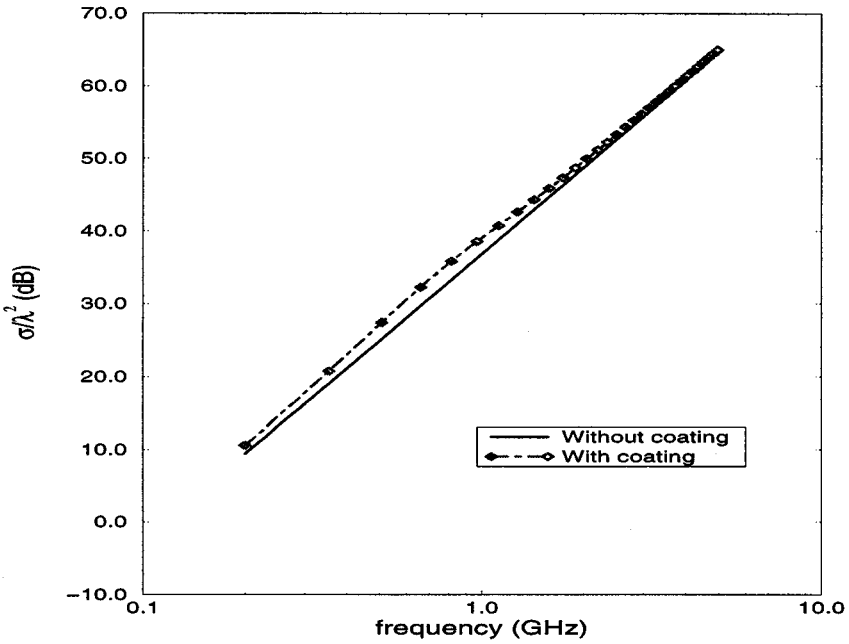

Fig. 10. Bistatic RCS of the conducting sphere (E-plane) in the deep shadow region ($\theta = 0^\circ$), without and with coating [Table IV(b)]. (Diameter of the sphere varies between $1\ \lambda - 10\lambda$ in the optimized frequency range of 0.2–2 GHz.)

and cannot reduce the bistatic RCS in the deep shadow region. The bistatic RCS in the H-plane has almost the same behavior as the E-plane. Note that, as expected, in the lit region the bistatic RCS follows the same GO formula as in (8).

V. GA Technique with Hybrid Planar/Curved Surface Implementation

This section focuses on designing an optimal RAM coating for the curved surfaces using the GA technique via a hybrid planar/curved surface population initialization. In general, obtaining the optimal coating for the curved surfaces compared to the planar structures is more complex and much more time consuming. Clearly seeking an efficient optimization procedure for curved surfaces is desirable. For instance, the computer run time in obtaining the reflection coefficient of the coated planar structure on an HPC-180 workstation is about 0.0006 s, while the RCS of the coated spherical structure is obtained in about 0.252 s. This shows that there is a huge computational time difference in synthesizing the wide-band absorbing materials for spherical structure compared to the planar structure. This section investigates the question of the effectiveness of using the best population for the planar RAM as the initial population in the GA technique in designing an optimal RAM for curved surfaces.

Fig. 11 shows the RCS of a conducting sphere coated with the optimal planar coating [Table II(a)] and compares it with the RCS of a sphere coated with the optimum spherical coating [Table IV(a)]. It is observed that the optimized coating corresponding to the planar structure creates an almost the same characteristic as with the optimal spherical coating and reduces the RCS of the spherical structure considerably. Note that the optimal planar coating on the HPC-180 workstation is achieved in about 1 min, while it takes approximately 7 hr to obtain the optimal spherical coating on this workstation. This computational time is for evaluating the RCS for 100 generations (initial population was randomly selected), included 100 individuals per generation, at ten different frequency points (i.e., 10^5 RCS computations). The convergence curve for this optimization process is shown in Fig. 12. It is observed that it takes nearly 40 generations before the convergence curve approaches the final result.

Next, the GA optimizer is initiated using as its initial population the best population obtained from the optimal design of the planar structure to design the optimal spherical coating as represented in Table V. The convergence curve for this implementation is also shown in Fig. 12. It is clearly observed that the optimization process requires significantly less number of generations to approach the final design. As expected due to the inherent robustness of the GA optimizer, no matter what the initial population the final optimal result is almost independent of the initial population. However, starting with a better initial population one can expedite the convergence rate noticeably. Fig. 11 compares RCS of RAM coated sphere using various schemes as discussed above.

These observations may suggest that the optimal coating for an arbitrary shaped structure may be obtained by first analyzing the multilayered planar structure and determining the best population for minimizing its reflection coefficient. Next, this population should be used as the initial population for the GA optimizer applied to the curved surfaces to allow for rapid determination of the optimal coating for the curved structures.

VI. Conclusion

In this paper, a novel procedure for synthesizing RAM in a wide-band frequency range for reducing RCS of curved tar-

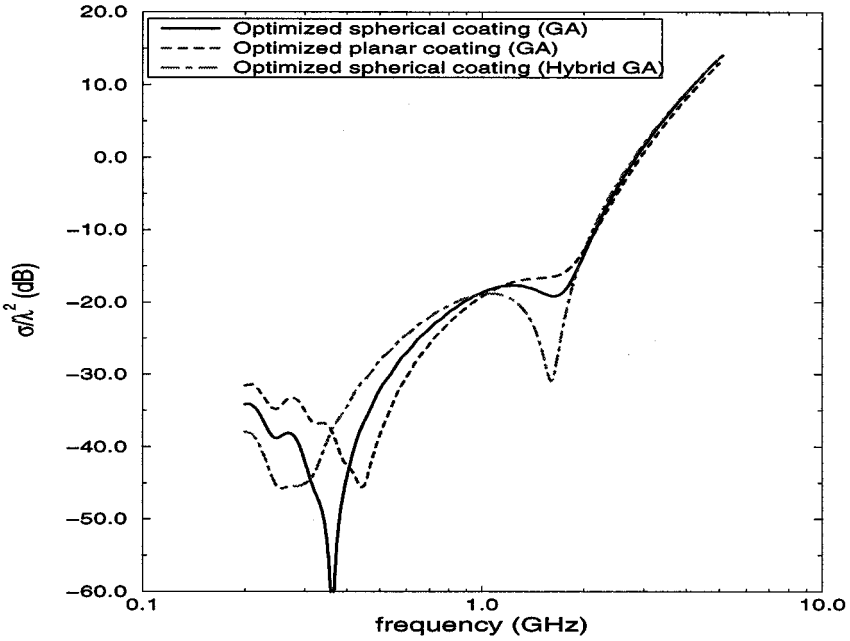

Fig. 11. Comparison of the RCS of the conducting sphere coated with the optimal spherical coating [Table IV(a)], optimal planar coating [Table II(a)], and optimal spherical coating using GA hybrid planar/curved surface implementation (Table V). (Diameter of the sphere varies between $1\ \lambda - 10\ \lambda$ in the optimized frequency range of 0.2–2 GHz.)

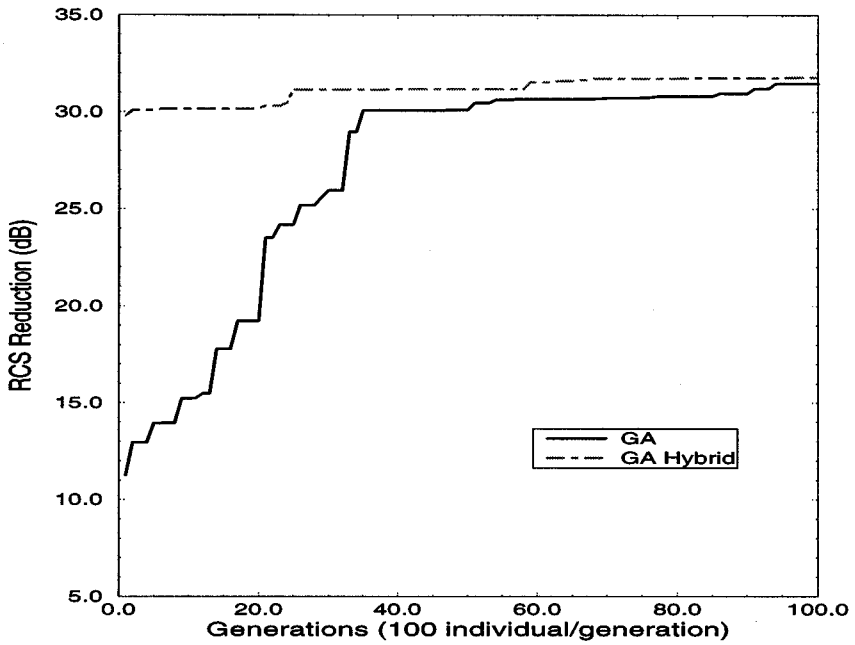

Fig. 12. Convergence curve of the GA hybrid planar/curved surface implementation compared to the GA method for RCS reduction of the conducting sphere. (Diameter of the sphere varies between $1\ \lambda - 10\ \lambda$ in the optimized frequency range of 0.2–2 GHz.)

gets is presented. Multilayered planar, cylindrical, and spherical canonical structures are analyzed using the modal solutions of Maxwell's equations. Subsequently, the GA optimization technique is integrated with the modal solutions to obtain the optimal absorbing materials for RCS reduction. Since the GA produces the global solution without requiring much information about the solution domain, it has been found to be a very effective method for obtaining the optimal coating. An in-depth study was performed to evaluate the potential usage of the optimal planar coating as applied to the curved surfaces. It is observed

TABLE V
OPTIMUM RAM DESIGNED BY GA HYBRID PLANAR/CURVED SURFACE IMPLEMENTATION FOR THE 148 CM DIAMETER CONDUCTING SPHERE. (MONOSTATIC CASE) $(0.2 \leq f_{\text{opt}}(\text{GHz}) \leq 2)$

Layer	Material #	$t\,(cm)$
1	15	0.0954
2	6	0.177
3	4	0.0741
4	4	0.156
5	4	0.159

that the optimal planar coating can noticeably reduce RCS of curved structures. This observation was essential in introducing a novel efficient GA implementation using as part of its initial generation the best population obtained for the planar RAM design. These results suggest that the optimal RAM for a surface with an arbitrary curvature may be determined by applying the GA technique.

It is shown that for the structures studied in this paper by a proper composition of absorbing materials, the monostatic RCS of the planar, cylindrical, and spherical conducting structures is reduced about 27 dB in the optimization frequency range of 0.2–2 GHz. In the resonance region, the coating absorbs the energy of the incident wave strongly; however, as one extends to the Rayleigh region the finite conductivity of some of the RAM makes the coating act like a perfect conductor and the RCS cannot be reduced as effectively as in the resonance region. Around the geometrical optics region, the relative permittivity and permeability of the materials are decreased and the coating cannot control the RCS of the structure effectively.

The bistatic RCS reduction of the coated conducting cylindrical and spherical structures has also been investigated. It has been observed that, although the optimal coating was achieved for reducing the monostatic RCS, due to the existence of loss, it has also reduced the bistatic RCS in the lit region. In the deep shadow region no matter which type of coating is used the scattered field is almost 180° out of phase with the incident wave. Therefore, the optimal RAM only increases the size of the structure and cannot reduce the bistatic RCS.

In addition, the effectiveness of the optimal planar coating in designing the optimal RAM for the curved surfaces is investigated. It has been shown that the optimal planar coating has almost the same effect as the optimal spherical coating in reducing the monostatic RCS of spherical structures. Additionally, the best population for the planar coating is integrated as the initial population for an efficient GA technique to obtain the optimal coating for the spherical structure. It has been shown that this implementation of GA has a very fast convergence rate. This suggests that for the sake of the computational time reduction, the optimal RAM for curved surfaces can be obtained using the GA technique with the hybrid planar/curved strategy.

REFERENCES

[1] H. C. Strifors and G. C. Gaunaurd, "Scattering of electromagnetic pulses by simple-shaped targets with radar cross section modified by a dielectric coating," *IEEE Trans. Antennas Propagat.*, vol. 46, pp. 1252–1262, Sept. 1998.

[2] E. Michielssen, J. M. Sajer, S. Ranjithan, and R. Mittra, "Design of lightweight, broad-band microwave absorbers using genetic algorithms," *IEEE Trans. Microwave Theory Tech.*, vol. 41, pp. 1024–1031, June/July 1993.

[3] D. S. Weile, E. Michielssen, and D. E. Goldberg, "Genetic algorithm design of pareto optimal broad-band microwave absorbers," *IEEE Trans. Electromagnetic Compatibility*, vol. 38, pp. 518–524, Aug. 1996.

[4] B. Chambers and A. Tennant, "Optimized design of Gaumann radar absorbing materials using a genetic algorithm," *Proc. Inst. Elect. Eng. Radar, Sonar, Navigat.*, vol. 143, no. 1, pp. 23–30, Feb. 1996.

[5] Y. Rahmat-Samii and E. Michielssen, *Electromagnetic Optimization by Genetic Algorithms*. New York: Wiley, 1999.

[6] J. R. Wait, *Electromagnetic Waves in Stratified Media*, 2nd ed. New York, NY: Pergamon, 1970.

[7] ——, *Electromagnetic Probing in Geophysics*. Boulder, CO: Golem, 1971.

[8] ——, *Geoelectromagnetism*. New York: Academic, 1982.

[9] ——, "Electromagnetic scattering from a wire grid parallel to a planar stratified medium," *IEEE Trans. Antennas Propagat.*, vol. AP-20, pp. 672–675, Sept. 1972.

[10] J. R. Wait and D. C. Chang, "Theory of electromagnetic scattering from a layered medium with a laterally varying substrate," *Radio Sci.*, vol. 11, no. 3, pp. 221–229, Mar. 1976.

[11] B. A. Beartlein, J. R. Wait, and D. G. Dudley, "Scattering by a conducting strip over a lossy half-space," *Radio Sci.*, vol. 24, no. 4, pp. 485–497, July/Aug. 1989.

[12] J. R. Wait, "Fields of a horizontal wire antenna over a layered half-space," *J. Electromagn. Waves Appl.*, vol. 10, no. 12, pp. 1655–1662, 1996.

[13] ——, "The ancient and modern history of EM ground-wave propagation," *IEEE Antennas Propagat. Mag.*, vol. 40, pp. 7–24, Oct. 1998.

[14] ——, *Electromagnetic Radiation from Cylindrical Structures*. New York: Pergamon, 1959.

[15] ——, "Scattering of plane wave from a circular dielectric cylinder at oblique incidence," *Can. J. Phys.*, vol. 33, no. 5, pp. 189–195, May 1955.

[16] ——, "Electromagnetic response of an anisotropic conducting cylinder to an external source," *Radio Sci.*, vol. 13, no. 5, pp. 789–792, Sept./Oct. 1978.

[17] J. R. Wait and D. A. Hill, "Theory of transmission of electromagnetic waves along a drill rod in conducting rock," *IEEE Trans. Geosci. Electron.*, vol. 17, no. 2, pp. 21–24, Apr. 1979.

[18] J. R. Wait and R. L. Gardner, "Electromagnetic nondestructive testing of cylindrically layered conductors," *IEEE Trans. Instrum. Meas.*, vol. IM-28, pp. 159–161, June 1979.

[19] J. R. Wait and D. A. Hill, "Dynamic electromagnetic response of a homogeneous conducting cylinder for symmetric excitation," *Appl. Phys.*, vol. 20, no. 1, pp. 89–96, Sept. 1979.

[20] J. R. Wait, "Exact surface impedance for a cylindrical conductor," *Electron. Lett.*, vol. 15, no. 20, pp. 659–660, Sept. 1979.

[21] ——, "General formulation of the induction logging problem for concentric layers about the borehole," *IEEE Trans. Geosci Remote Sens.*, vol. GRS-22, pp. 34–42, Jan. 1984.

[22] ——, "Impedance conditions for a coated cylindrical conductor," *Radio Sci.*, vol. 21, no. 4, pp. 623–626, July/Aug. 1986.

[23] C. J. Rodger, J. R. Wait, and R. L. Dowden, "Electromagnetic scattering from a group of thin conducting cylinders," *Radio Sci.*, vol. 32, no. 3, pp. 907–912, May/June 1997.

[24] J. R. Wait, "Electromagnetic scattering from a radially inhomogeneous sphere," *Appl. Sci. Res. B*, vol. 10, no. 5/6, pp. 441–450, 1963.

[25] ——, "Electromagnetic transient response of a spherical conducting shell," *Electron. Lett.*, vol. 4, no. 26, pp. 576–577, Dec. 1968.

[26] ——, "Electromagnetic induction in solid conducting sphere enclosed by a thin conducting spherical shell," *Geophys.*, vol. 34, no. 5, pp. 753–759, Oct. 1969.

[27] D. A. Hill and J. R. Wait, "Electromagnetic scattering of a small spherical obstacle near the ground," *Can. J. Phys.*, vol. 50, no. 3, pp. 237–243, Feb. 1972.

[28] J. R. Wait, "Exact surface impedance for a spherical conductor," *Proc. IEEE*, vol. 68, no. 2, pp. 279–281, Feb. 1980.

[29] ——, *Wave Propagation Theory*. New York: Pergamon, 1981.

[30] J. M. Johnson and Y. Rahmat-Samii, "Genetic algorithms in engineering electromagnetics," *IEEE Antennas Propagat. Mag.*, vol. 39, pp. 7–21, Aug. 1997.

[31] D. S. Weile and E. Michielssen, "Genetic algorithm optimization applied to electromagnetics: A review," *IEEE Trans. Antennas Propagat.*, vol. 45, pp. 343–353, Mar. 1997.

[32] D. L. Carroll, *Fortran Genetic Algorithm Driver*. Urbana, IL: Univ. Illinois Urbana-Champaign, 1997.
[33] M. Abramowitz and I. A. Stegun, *Handbook of Mathematical Functions with Formulas, Graphs, and Mathematical Tables*, 9th ed. New York: Dover, 1972.
[34] D. E. Amos, *A Subroutine Package for Bessel and Hankel Functions of Complex Arguments*. Albuquerque, NM: Sandia Nat. Labs., 1996.
[35] D. J. Hoppe and Y. Rahmat-Samii, *Impedance Boundary Conditions in Electromagnetics*: Taylor Francis, 1995.
[36] R. E. Hiatt, K. M. Siegel, and H. Weil, "The ineffectiveness of absorbing coatings on conducting objects illuminated by long wavelength radar," *Proc. IRE*, vol. 48, pp. 1636–1642, Sept. 1960.
[37] A. Ishimaru, *Electromagnetic Wave Propagation, Radiation, and Scattering*. Englewood Cliffs, NJ: Prentice-Hall, 1991.

Hossein Mosallaei (S'98) received the B.Sc. and M.Sc. degrees in electrical engineering from Shiraz University, Shiraz, Iran, in 1991 and 1995, respectively. He is currently working toward the Ph.D. degree in the electrical engineering department at the University of California, Los Angeles (UCLA).

Since 1997, he has been working both as a Graduate Research Assistant in the UCLA Antenna Laboratory and as a Teaching Associate. His research interests include computational electromagnetics, waves interaction in complex media, photonic bandgap structures, antenna design, and genetic algorithm.

Yahya Rahmat-Samii (S'73–M'75–SM'79–F'85) received the M.S. and Ph.D. degrees in electrical engineering from the University of Illinois, Urbana-Champaign.

He is a Professor of electrical engineering at the University of California, Los Angeles (UCLA). He was a Senior Research Scientist at NASA's Jet Propulsion Laboratory/California Institute of Technology before joining UCLA. He was a Guest Professor at the Technical University of Denmark (TUD) in the summer of 1986. He has also been a Consultant to many aerospace companies. He has been Editor and Guest Editor of many technical journals and book publication entities. He has authored and coauthored over 450 technical journal articles and conference papers and has written 14 book chapters. He is the coauthor of *Electromagnetic Optimization by Genetic Algorithms* (New York: Wiley, 1999), and *Impedance Boundary Conditions in Electromagentics* (Washington, DC: Taylor Francis, 1995). He is also the holder of several patents. He has had pioneering research contributions in diverse areas of electromagnetics, antennas, measurement and diagnostics techniques, numerical and asymptotic methods, satellite and personal communications and human/antenna interactions, etc. (visit http://www.antlab.ee.ucla.edu).

Dr. Rahmat-Samii was the 1995 President and 1994 Vice-President of IEEE Antennas and Propagation Society. He was appointed an IEEE Antennas and Propagation Society Distinguished Lecturer and presented lectures internationally. He was elected as a Fellow of IAE in 1986. He was a member of the Strategic Planning and Review Committee (SPARC) of IEEE. He has been the Guest and Plenary Session Speaker at many national and international symposia. He was one of the Directors and Vice President of the Antennas Measurement Techniques Association (AMTA) for three years. He has also served as Chairman and Co-Chairman of several national and international symposia. He was also a member of UCLA's Graduate council for a period of three years. For his contributions, he has received numerous NASA and JPL Certificates of Recognition. In 1984, he was the recipient of the prestigious Henry Booker Award of URSI. In 1992 and 1995, he was the recipient of the Best Application Paper Award (Wheeler Award) for papers published in the 1991 and 1993 IEEE TRANSACTIONS ON ANTENNAS AND PROPAGATION. He is a member of Commissions A, B, J, and K of USNC/URSI, AMTA, Sigma Xi, Eta Kappa Nu, and the Electromagnetics Academy. He is listed in *Who's Who in America*, *Who's Who in Frontiers of Science and Technology*, and *Who's Who in Engineering*. In 1999, he was the recipient of the University of Illinois ECE Distinguished Alumni Award. In 2000, he was selected as the recipient of IEEE Third Millennium Medal and the AMTA 2000 Distinguished Achievement Award.